Proceedings of

Factory Automation 2010

15-16th April, 2010
Kecskemét, Hungary

Content

Approximation Algorithm for the Force of Pneumatic Artificial Muscles

JÓZSEF SÁROSI[1], TAMÁS SZÉPE[2], JÁNOS GYEVIKI[3]
[1]Department of Technical and Process Engineering, Faculty of Engineering, University of Szeged, Mars tér 7, Szeged, H-6724, HUNGARY
[1]sarosi@mk.u-szeged.hu
[2]Department of Computer Algorithms and Artificial Intelligence, Faculty of Science and Informatics, University of Szeged, Árpád tér 2, Szeged, H-6720, HUNGARY
[2]szepet@inf.u-szeged.hu
[3]Department of Technical and Process Engineering, Faculty of Engineering, University of Szeged, Mars tér 7, Szeged, H-6724, HUNGARY
[3]gyeviki@mk.u-szeged.hu

Abstract: - Many researchers have tried to introduce several mathematical models for pneumatic artificial muscle (PAM). However, we have found significant differences between the theoretical and experimental results. In this paper we present our new approximation algorithm for the force of PAM, comparing with measured and literary data.

Key-Words: - Pneumatic artificial muscle, approximation algorithms, MATLAB

1 Introduction

The braided pneumatic actuator was invented by physician Joseph L. McKibben in the 1950's. This type of actuators is powered by compressed air. Many researchers have investigated and improved the characteristics of PAMs.

The working principle of the pneumatic artificial muscles is well described in literature [1], [2], [3], [4] and [5].

Pneumatic artificial muscles can be used as an actuator in robotics and prostheses because it has big power and is soft in material and motion. Due to their highly nonlinear and time-varying nature pneumatic muscles are difficult to control [6].

Pneumatic muscle actuators consist of a rubber bladder enclosed within a helical braid that is clamped on both ends (Fig. 1 and Fig. 2). As the bladder is pressurized, its volume increases and the braid and clamps act to shorten the overall length of the actuator [7].

Figure 1. Fluid Muscles made by Festo

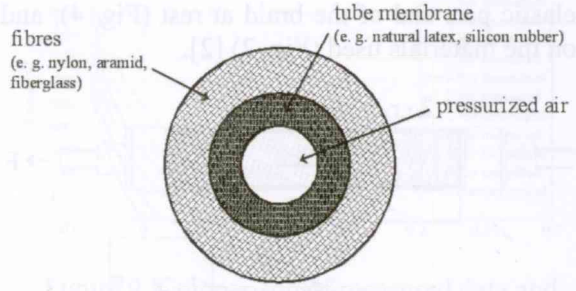

Figure 2. Orthotropic material layers of PAM

To find the relationship of the tension, length (contraction) and pressure, some theoretical approaches and experiments have been analyzed. The Fluid Muscle DMSP-10-250N-RM-RM (with inner diameter of 10 mm and initial length of 250 mm) produced by Festo company is selected for our newest study.

The layout of this paper is as follows. Section 2 (Materials and Methods) is devoted to display our test-bed for investigation of pneumatic muscle and to demonstrate the model of force as a function of pressure and length (contraction). Section 3 (Results and Discussion) presents several experimental results and gives some comparisons for measured and literary data. Finally, section 4 (Conclusions and Future Work) gives the investigations we plan.

2 Materials and Methods

Good descriptions of our test-bed (Fig. 3) and experimental results can be found in [8] and [9].

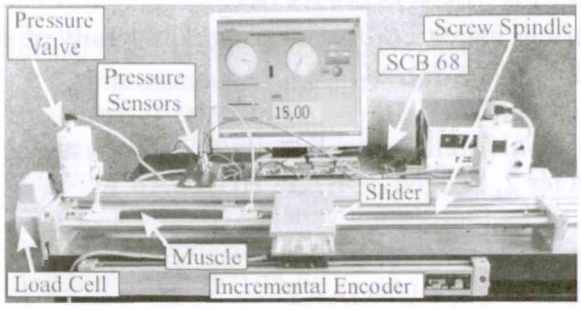

Figure 3. Experimental setup for investigations of PAMs

With the help of this setup several static and dynamic investigations and control methods can be carried out.

The general behaviour of PAM with regard to shape, contraction and tensile force when inflated depends on the geometry of the inner elastic part and of the braid at rest (Fig. 4), and on the materials used (Fig. 2) [2].

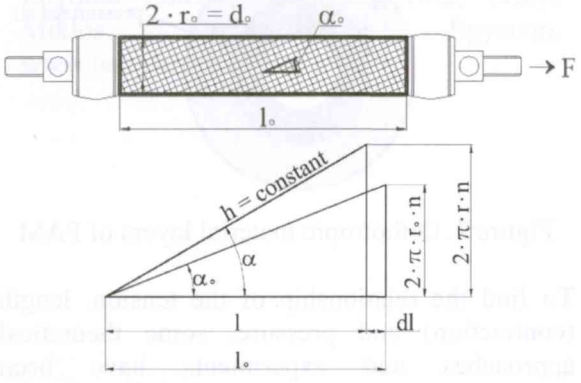

Figure 4. Geometry parameters of PAM

On the basis of [3], [10] and Fig. 4, the force can be calculated:

$$F(p,\kappa) = \pi \cdot p \cdot r_0^2 \cdot (a \cdot (1-\kappa)^2 - b) \qquad (1)$$

$$a = \frac{3}{tg^2\alpha_0} \qquad \frac{1}{\sin^2\alpha_0} \qquad \kappa = \frac{l_0 - l}{l_0}$$

Where: F the pulling force, p the applied pressure, r_0, l_0, α_0 the initial inner radius and length of the PAM and the initial angle between the thread and the muscle long axis, r, l, α the inner radius and length of the PAM and angle between the thread and the muscle long axis when the muscle is contracted, h the constant thread length, n the number of turns of thread and κ the contraction.

Equation 1 is based on the admittance of a continuously cylindrical-shaped muscle. The fact is that the shape of the muscle is not cylindrical on the end, but rather is flattened, accordingly, the more the muscle contracts, the more its active part decreases, so the actual maximum contraction ration is smaller than expected.

Tondu and Lopez in [3] consider improving equation 1 with a correction factor (ε), on the one hand, it does not pay attention to the material that the muscle is made of, and on the other hand, it predicts for various pressures the same maximal contraction. This new equation is relatively good for higher pressure ($p \geq 2$ bar). Kerscher et al. in [10] suggest achieving similar approximation for smaller pressure another correction factor (μ) is needed, so the modified equation is:

$$F(p,\kappa) = \mu \cdot \pi \cdot p \cdot r_0^2 \cdot (a \cdot (1-\varepsilon \cdot \kappa)^2 - b) \qquad (2)$$

$$\varepsilon = a_\varepsilon \cdot e^{-p} - b_\varepsilon \qquad \mu = a_\kappa \cdot e^{-\kappa \cdot 40} - b_\kappa$$

3 Results and Discussion

Tensile force of artificial muscle under different constant pressures is a function of muscle length (contraction) and of air pressure. The force always drops from its highest value at full muscle length to zero at full inflation and position (Fig. 5).

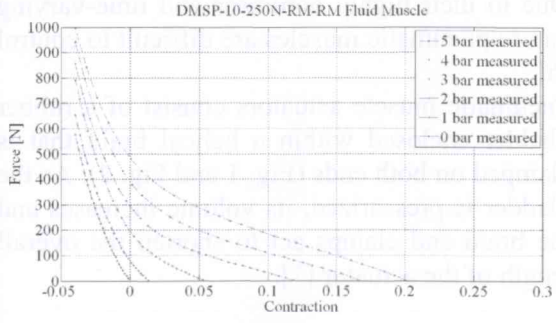

Figure 5. Isobaric force-contraction diagram of Fluid Muscle

Next, we compared the measured data and force model using equation 1.

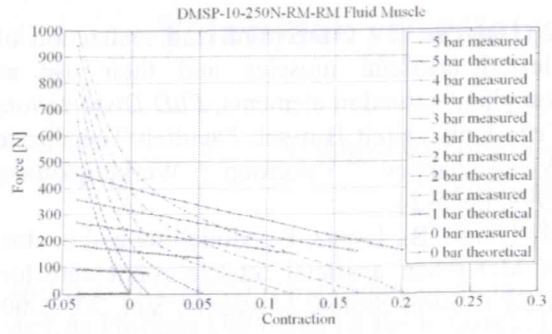

Figure 6. Comparison of measured data and force model using equation 1

As it is shown in Fig. 6, there is only one intersection between the measured and calculated results and no fitting.

In the interest of fitting we repeated the simulation with equation 2. The coefficients (a_ε, b_ε, a_κ and b_κ) of equation 2 were found using genetic algorithm in MATLAB (Fig. 7).

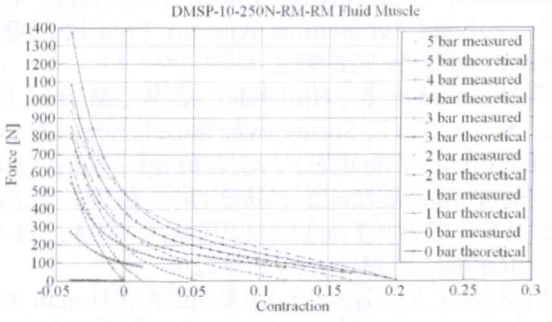

Figure 7. Comparison of measured data and force model using equation 2

Fig. 7 shows the measured and predicted results still do not fit, for this reason we had to widen the search parameters of the genetic algorithm. With the help of it, a better fitting was attained (Fig. 8), but at a pressure of 0 Bar we still have a rather substantial inconsistency.

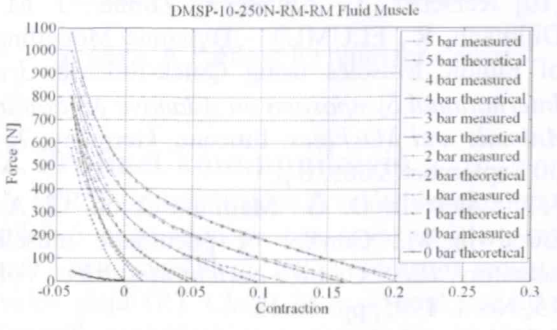

Figure 8. Comparison of measured data and force model using equation 2 with the widening of the search parameters

In the interest of better fitting under different pressures including 0 Bar we have introduced a new approximation algorithm:

$$F(\kappa) = a \cdot e^{(b \cdot \kappa + c)} + d \cdot \kappa + e \qquad (3)$$

Under fixed pressure the contraction to force function can be approximated with a general exponential function with first order correction polynomials of contraction.
To make our equation 3 universal meaning usable under various pressures we need to make the algorithm vary from pressure:

$$F(p, \kappa) = (a \cdot p + b) \cdot e^{(c \cdot \kappa + d)} + (e \cdot p + f) \cdot \kappa + g \cdot p + h \qquad (4)$$

The unknown *a, b, c, d, e, f, g* and *h* parameters can be found using genetic algorithm, too.

The fitting with the 8 parameters received from the algorithm can be seen in Fig. 9.

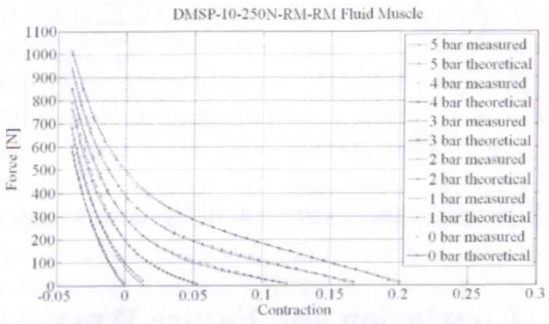

Figure 9. Comparison of measured data and force model using equation 4

As we can see we have consistent fitting even at a pressure of 0 Bar.

Numbers have investigated the precise position control of pneumatic muscles during the past several years [3], [6], [11] and [12]. Most of them dealt with the control of single or antagonistic pneumatic muscles. The positioning of PAMs requires accurate determination of the dynamic model of pneumatic actuators. With the help our test-bed the hysteresis can be accurately predicted. Chou and Hannaford in [12] report hysteresis to be substantially due to Coulomb friction, which is caused by the contact between the bladder and the shell, between the braided threads and each other, and the shape changing of the bladder. An experiment was made to illustrate the hysteresis (Fig. 10).

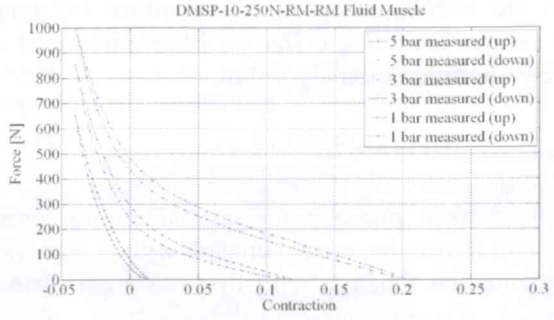

Figure 10. Hysteresis in the tension-length (contraction) cycle

To prove versatility of equation 4, another comparison was done between the measured data and force model. The accurate fitting is demonstrated in Fig. 11.

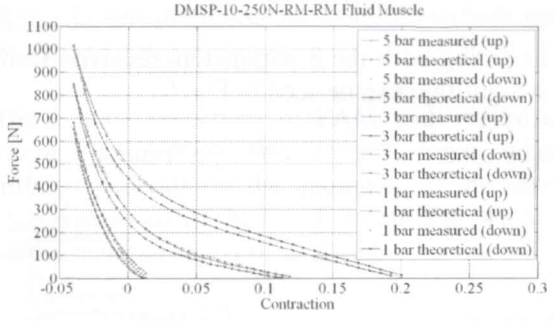

Figure 11. Approximation of hysteresis loop

4 Conclusion and Future Work

In this work a comparison of theoretical and measured forces generated by pneumatic artificial muscle has been shown. As we can see there is a substantial difference between the measured and predicted forces, for this reason we had to develop a radically new equation based on purely statistical approach. With the help of it precise curve fitting can be proven for any fluid muscles. Our goal is to develop a new mathematical model for pneumatic artificial muscles on the basis of our approximation model and to construct a prosthetic arm with PAMs, because these muscles seem a better choice than present day electric or other drives.

References:

[1] Caldwell, D. G., Razak, A., Goodwin, M. J., Braided pneumatic muscle actuators, *Proceedings of the IFAC Conference on Intelligent Autonomous Vehicles*, Southampton, United Kingdom, 18-21 April, 1993, pp. 507-512.

[2] Daerden, F., Conception and realization of pleated artificial muscles and their use as compliant actuation elements, *PhD Dissertation*, Vrije Universiteit Brussel, Faculteit Toegepaste Wetenschappen Vakgroep Werktuigkunde, 1999, pp. 5-24.

[3] Tondu, B., Lopez, P., Modelling and control of McKibben artificial muscle robot actuator, *IEEE Control System Magazine*, Vol. 20, 2000, pp. 15-38.

[4] Daerden, F., Lefeber, D., Pneumatic artificial muscles: actuator for robotics and automation, *European Journal of Mechanical and Environmental Engineering*, Vol. 47, 2002, pp. 10-21.

[5] Balara, M., Petík, A., The properties of the actuators with pneumatic artificial muscles, *Journal of Cybernetics and Informatics*, Vol. 4, 2004, pp. 1-15.

[6] Situm, Z., Herceg, Z., Design and control of a manipulator arm driven by pneumatic muscle actuators, *16th Mediterranean Conference on Control and Automation*, Ajaccio, France, 25-27 June, 2008, pp. 926-931.

[7] Bharadwaj, K., Hollander, K. W., Mathis, C. A., Sugar, T. G., Spring over muscle actuator for rehabilitation devices, *Proceedings of the 26th Annual International Conference of the IEEE EMBS*, San Francisco, CA, USA, 1-4 September, 2004, pp. 2726-2729.

[8] Sárosi J., Gyeviki J., Véha A., Toman P., Accurate position control of PAM actuator in LabVIEW environment, *IEEE, 7th International Symposium on Intelligent Systems and Informatics*, Subotica, Serbia, 25-26 September, 2009, pp. 301-305.

[9] Sárosi, J., Gyeviki, J., Szabó, G., Szendrő P., Laboratory investigations of fluid muscles, *Annals of Faculty of Engineering Hunedoara, International Journal of Engineering*, 2010, Vol. 8, No. 1, pp. 137-142.

[10] Kerscher, T., Albiez, J., Zöllner, J. M., Dillmann, R., FLUMUT - Dynamic Modelling of Fluidic Muscles using Quick-Release, *3rd International Symposium on Adaptive Motion in Animals and Machines*, Ilmenau, Germany, 25-30 September, 2005, 6 p.

[11] Caldwell, D. G., Medrano-Cerda, G. A., Goodwin M., Control of pneumatic muscle actuators, *IEEE Control System Magazine*, Vol. 15, No. 1, 1995, pp. 40-48.

[12] Chou, C. P., Hannaford, B., Measurement and modeling of McKibben pneumatic artificial muscles, *IEEE Transactions on Robotics and Automation*, Vol 12, No. 1, 1996, pp. 90-102.